© 2004 The Chemical Society of Japan

Selected Paper

The Magnetic Susceptibilities and Electron Paramagnetic Resonance Spectra of 6H-Perovskites $Ba_3PrM_2O_9$ (M = Ir, Ru)

Yukio Hinatsu,* Shigeaki Oyama, and Yoshihiro Doi

Division of Chemistry, Graduate School of Science, Hokkaido University, Sapporo 060-0810

Received March 26, 2004; E-mail: hinatsu@sci.hokudai.ac.jp

The magnetic properties of quaternary oxides $Ba_3PrM_2O_9$ and $Ba_3CeM_2O_9$ (M = Ir, Ru) have been investigated. They crystallize in the 6H-perovskite structure with the space group $P6_3/mmc$, in which the cation sites with the face-sharing octahedra are occupied by Ir (or Ru) ions, and those within the corner-sharing octahedra are occupied by Pr (or Ce) ions. Magnetic susceptibility measurements for $Ba_3PrIr_2O_9$ show that an antiferromagnetic interaction between two Ir ions in the Ir_2O_9 dimer results in a large temperature-independent paramagnetic susceptibility over a wide temperature range. Another interesting result is in the small effective magnetic moments for $Ba_3PrIr_2O_9$ (0.31(1) μ_B) and for $Ba_3PrRu_2O_9$ (0.75(1) μ_B). The electron paramagnetic resonance (EPR) spectrum of Pr^{4+} in these compounds was measured by diluting them in the corresponding isomorphous compounds $Ba_3CeIr_2O_9$ and $Ba_3CeRu_2O_9$ and lowering the temperature to 4.2 K. A very large hyperfine interaction with the ^{141}Pr nucleus was observed. The results were analyzed based on the weak field approximation. The measured g values are much smaller than $|-10/7|$, showing that the crystal field effect on the behavior of a 4f electron is large. The low g values correspond to the small effective magnetic moments of the Pr compounds.

The most stable oxidation state of lanthanides is trivalent. In addition to this state, cerium, praseodymium, and terbium have the tetravalent state.[1] Nonetheless, there are surprisingly few compounds in which praseodymium or terbium is exclusively tetravalent. Furthermore, very little magnetic data have been published for tetravalent praseodymium compounds, despite its straightforward $4f^1$ electronic configuration. One of the most challenging problems in the modern chemistry of lanthanide compounds is to prepare compounds containing tetravalent praseodymium ions and to find magnetic cooperative phenomena which are ascribable to the behavior of unpaired 4f electrons.

We have been focusing our attention on the perovskite-type compounds. The lanthanide ion is relatively large and tends to adopt a high coordination number. Therefore, the lanthanide ion usually sits at the A site of the perovskite-type oxide ABO_3. By selecting large alkaline earth elements such as Sr and Ba as the A site atoms, one finds that lanthanides occupy the 6-coordinate B sites, i.e., the structure can be described as a framework of corner shared LnO_6 octahedra. The B site ions normally determine the physical properties of the perovskites ABO_3. Previously, we investigated the crystal structures and magnetic properties of many ABO_3-type perovskites containing lanthanide ions at the B-site.[2–8] Among them, it is noteworthy that $BaPrO_3$, $SrTbO_3$, and $BaTbO_3$ show antiferromagnetic transitions at relatively high temperatures, i.e., 11.5, 32.0, and 33.4 K, respectively.[2,3,6]

Now, our studies extend to perovskite-type oxides containing both the lanthanides (Ln) and platinum group metals (M) at the B sites. Highly oxidized cations from the second or third transition series sometimes show quite unusual magnetic behavior. In general, perovskites have some flexibility in chemical composition and crystal structure. When the ratio of the Ln and M ions is 1:2, such compounds often adopt a hexagonal perovskite structure. The 6H-$BaTiO_3$ type structure is most likely.[9] In this structure, there exist two kinds of sites for the B ions: the corner-sharing octahedral site and the face-sharing octahedral site. Generally, a B site ion with a large size and a low oxidation state occupies the former kind of site, and that with a small size and a high oxidation state occupies the latter kind of site. In the case of $Ba_3LnM_2O_9$, Ln and M ions occupy the corner-sharing and face-sharing sites, respectively, and form the LnO_6 octahedron and the M_2O_9 polyhedron (MO_6 dimer).

Previously, we reported a series of 6H-perovskites, $Ba_3LnRu_2O_9$, and investigated their magnetic properties.[10–12] For Ln = Ce, Pr, and Tb, they adopt the valence configuration of $Ba_3Ln^{4+}Ru^{4+}{}_2O_9$, and show a characteristic temperature-dependence of the magnetic susceptibilities. That is, a broad maximum at high temperatures (~350 K) and a magnetic transition at 9–11 K, which reflects magnetic interactions between Ru ions in the Ru_2O_9 dimer and between Ln and Ru ions.[10]

Another interesting result is in the effective magnetic moment of $Ba_3PrRu_2O_9$. It was estimated to be 0.90 μ_B, which is much smaller than the free-ion magnetic moments of Pr^{4+} (2.54 μ_B),[10] but is close to the moments observed in the perovskites containing a Pr^{4+} ion in the octahedral site: 0.68 μ_B for $BaPrO_3$[2,4] and 0.812–0.879 μ_B for $Ba_{1-x}Sr_xPrO_3$.[13]

To clarify the nature of the peculiar temperature dependence of the magnetic susceptibility and the low effective magnetic moment of $Ba_3PrRu_2O_9$, we have performed two experiments in this study. First, we diluted $Ba_3PrRu_2O_9$ with $Ba_3CeRu_2O_9$ (Ce^{4+} is diamagnetic) and measured the electron paramagnetic resonance (EPR) spectrum of the Pr^{4+} ion to examine its electronic ground state. Furthermore, the corresponding iridium compound ($Ba_3PrIr_2O_9$) was prepared, and its magnetic susceptibility and EPR spectrum were measured. The Ir and Ru

Published on the web August 6, 2004; DOI 10.1246/bcsj.77.1479

Table 1. Lattice Parameters, Atomic Positional Parameters, and Some Bond Lengths for $Ba_3PrIr_2O_9$

$Ba_3PrIr_2O_9$	Space group $P6_3/mmc$ (No. 194), $Z = 2$, $a = 5.8939(2)$ Å, $c = 14.7014(4)$ Å			
Atom	Site	x	y	z	B/Å^2
Ba(1)	2*b*	0	0	1/4	0.44(2)
Ba(2)	4*f*	1/3	2/3	0.9021(1)	0.59(3)
Pr	2*a*	0	0	0	0.08(3)
Ir	4*f*	1/3	2/3	0.1637(1)	0.10(2)
O(1)	6*h*	0.4919(8)	0.9838	1/4	1.1(1)
O(2)	12*k*	0.1725(7)	0.3450	0.4134(5)	1.2(2)
Bond lengths					
Pr–O(2) × 6		2.174(7) Å	Ir–O(1) × 3		2.056(7) Å
Ir–Ir × 1		2.537(2) Å	Ir–O(2) × 3		1.995(7) Å

ions often produce the oxides with common crystal structures. However, their physical properties are sometimes quite different. The effects of Ir substitution for Ru in the face-sharing octahedral sites will provide us the information on the above-mentioned peculiar magnetic behavior. The results are discussed here.

Experimental

Sample Preparation. Two polycrystalline samples of $Ba_3PrIr_2O_9$ and $Ba_3CeIr_2O_9$ were prepared by firing the appropriate amounts of $BaCO_3$, Pr_6O_{11} (or CeO_2), and Ir metal powders, first at 900 °C for 12 h and then 1200 °C for several days in air with several interval grinding and pelleting steps. Specimens for EPR measurements, $Ba_3Pr_xCe_{1-x}M_2O_9$ ($x = 0.02$, 0.05; M = Ir, Ru), were also prepared. As starting materials, $BaCO_3$, Pr_6O_{11}, CeO_2, and Ir metal powders (or RuO_2) were used. The heating procedures were the same as the cases for $Ba_3PrIr_2O_9$ and $Ba_3CeIr_2O_9$. The progress of the reactions was monitored by powder X-ray diffraction measurements.

X-ray Diffraction Analysis. Powder X-ray diffraction profiles were measured using a Rigaku Multi-Flex diffractometer with Cu Kα radiation equipped with a curved graphite monochromator. The data were collected by step scanning in the angle range $10^\circ \leq 2\theta \leq 120^\circ$ at a 2θ step size of 0.04°. Crystal structures were determined by the Rietveld technique, using the program RIETAN.[14]

Magnetic Susceptibility Measurements. The temperature-dependence of the magnetic susceptibility was measured in an applied field of 0.1 T over the temperature range of 1.8 K $\leq T \leq$ 300 K using a SQUID magnetometer (Quantum Design, MPMS5S). The susceptibility measurements were performed under both the zero field cooling (ZFC) and field cooling (FC) conditions. The former was measured upon heating the sample to 300 K under the applied magnetic field of 0.1 T after zero-field cooling to 1.8 K. The latter was measured upon cooling the sample from 300 to 1.8 K at 0.1 T. There was no difference between the ZFC and FC susceptibilities in the whole experimental temperature range.

Specific Heat Measurements. The specific heats were measured using a relaxation technique through a specific heat measuring system (Quantum Design, PPMS) in the temperature range of 1.8 $\leq T \leq$ 300 K. The sample in the form of a thin plate was mounted on a sample holder with Apiezon for better thermal contact.

Electron Paramagnetic Resonance Measurements. The EPR measurements were carried out with a JEOL RE-2X spectrometer operating at an X-band frequency (9.1 GHz) with a 100-kHz field modulation. Measurements were made both at room temperature and at 4.2 K. The magnetic field was swept from 100 to 13500 G. Before the sample was measured, a blank was recorded to eliminate the possibility of interference from the background resonance of the cavity and/or sample tube. The magnetic field was monitored with a proton NMR gaussmeter, and the microwave frequency was measured with a frequency counter.

Results and Discussion

Crystal Structures. The X-ray diffraction measurements show that the $Ba_3PrIr_2O_9$ prepared in this study crystallizes in the 6H-perovskite type structure. The diffraction data were indexed in a hexagonal unit cell with the space group $P6_3/mmc$, and were analyzed by the Rietveld method. The lattice parameters, atomic positional parameters, and some important bond lengths are listed in Table 1. $Ba_3PrIr_2O_9$ is isostructural with $Ba_3PrRu_2O_9$[10,15,16] and its schematic structure is shown in Fig. 1.

Magnetic Susceptibilities. Figure 2(a) shows the temperature dependence of the magnetic susceptibility for $Ba_3PrIr_2O_9$. No magnetic anomaly was observed down to 1.8 K. The tem-

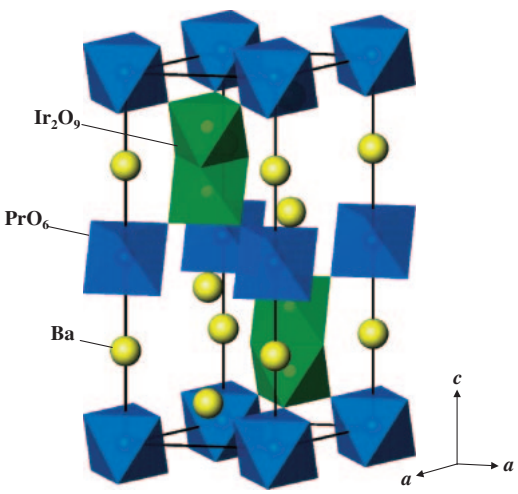

Fig. 1. The crystal structure of 6H-perovskite $Ba_3PrIr_2O_9$.

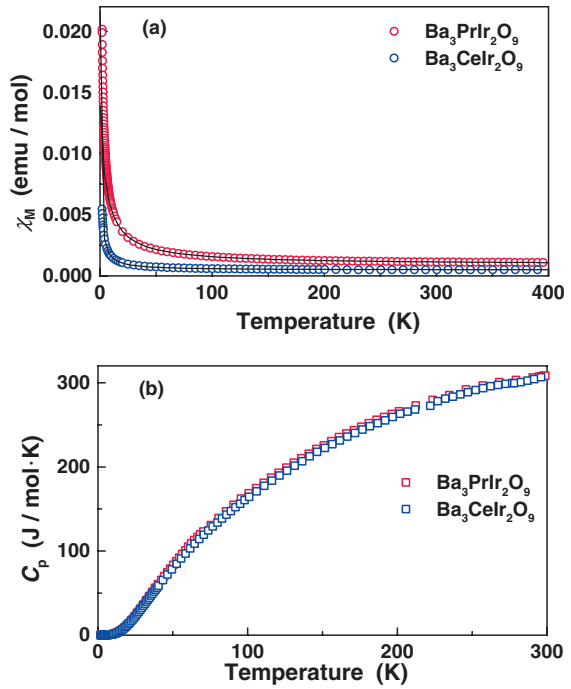

Fig. 2. Temperature dependence of (a) the magnetic susceptibility and (b) specific heat for $Ba_3PrIr_2O_9$ and $Ba_3CeIr_2O_9$. Solid lines in Fig. 2(a) show the modified Curie–Weiss law fitting.

perature dependence of the susceptibilities at higher temperatures ($T > 100$ K) is well fitted with the "modified" Curie–Weiss law in which the temperature independent paramagnetic susceptibility term (TIP) is included. The effective magnetic moment, the Weiss constant, and the TIP term were 0.75(1) μ_B, $-5.3(7)$ K, and 915×10^{-6} emu/mol, respectively. This effective magnetic moment is much smaller than the free-ion magnetic moment for Pr^{4+}, but is quite reasonable as the moment for a Pr^{4+} ion octahedrally coordinated by six oxygen ions, which we will discuss later using the results of the EPR measurements.

Specific Heats. Figure 2(b) shows the temperature dependence of the specific heat for $Ba_3PrIr_2O_9$. No anomaly was observed down to 1.8 K, which corresponds to the results of the magnetic susceptibility measurements.

We have already shown that the quaternary oxides $Ba_3LnRu_2O_9$ have the valence states $Ba_3Ln^{4+}Ru^{4+}{}_2O_9$ for Ln = Ce, Pr, and Tb from the X-ray diffraction measurements.[10] A similar valence configuration should be valid for the corresponding iridium compounds, which we reported as $Ba_3Ln^{4+}Ir^{4+}{}_2O_9$ for Ln = Ce, Pr, and Tb.[17]

In $Ba_3PrIr_2O_9$, both the magnetic moments of Pr^{4+} and Ir^{4+} contribute to the paramagnetism of the compound. In order to examine the magnetic contribution of the Pr^{4+} ion, a $Ba_3CeIr_2O_9$ compound in which the Ce^{4+} ions are substituted for the Pr^{4+} sites was prepared and its magnetic susceptibility was measured. The temperature dependence is also shown in Fig. 2(a). The susceptibility of $Ba_3CeIr_2O_9$ is much smaller than that of $Ba_3PrIr_2O_9$. It increases with decreasing temperature, but has a large temperature-independent term. The modified Curie–Weiss fitting gave the effective magnetic moment,

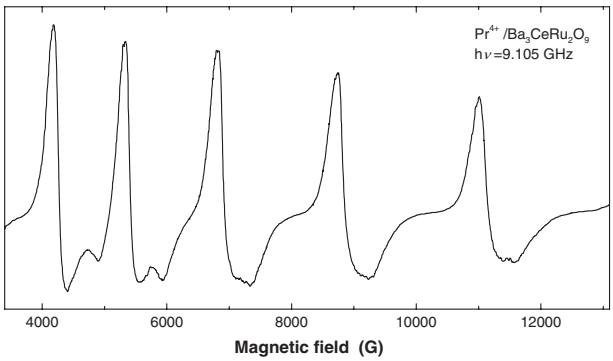

Fig. 3. An EPR spectrum for Pr^{4+} ion doped in $Ba_3CeIr_2O_9$ measured at 4.2 K.

the Weiss constant, and the TIP term as 0.31(1) μ_B, $-0.55(2)$ K, and $4.8(1) \times 10^{-4}$ emu/mol, respectively. We believe that this large TIP term is the result of the antiferromagnetic interaction between two Ir ions in the Ir_2O_9 dimer, and that the very small effective magnetic moment may be due to the existence of magnetically unpaired Ir ions formed by the small amount of oxygen defects. Comparing the effective magnetic moment for $Ba_3PrIr_2O_9$ with that for $Ba_3CeIr_2O_9$, we can conclude that the effective magnetic moment of $Ba_3PrIr_2O_9$ is due to the Pr^{4+} magnetic moment in this compound. In order to elucidate the small magnetic moment of Pr^{4+} in the $Ba_3PrIr_2O_9$, we have performed EPR measurements.

EPR Spectra. For the praseodymium ion in the tetravalent state, an EPR spectrum should be observed because the Pr^{4+} ion is a Kramers ion ([Xe]$4f^1$ configuration). However, no EPR spectra were observed, even at 4.2 K, for pure $Ba_3PrIr_2O_9$. Our previous study showed that the EPR spectra of the Pr^{4+} ion can be observed by diluting it in a nonmagnetic substance.[4,5,18] So, in this study we have prepared a sample in which the $Ba_3PrIr_2O_9$ is diluted with isomorphous $Ba_3CeIr_2O_9$. The ratio of Pr:Ce is 0.02:0.98 and 0.05:0.95. At low temperatures, EPR spectra could be observed. Figure 3 shows the spectrum measured at 4.2 K. This observation of an EPR spectrum strongly indicates that the oxidation state of the praseodymium ion is not trivalent, but tetravalent, because the non-Kramers Pr^{3+} ion usually shows no EPR spectrum.[19] There is no difference between two samples in which the concentrations of the Pr ions are different.

The tetravalent praseodymium Pr^{4+} is a Kramers' ion with one unpaired 4f electron and in a magnetic field one isotropic EPR spectrum may be observable. The isotope ^{141}Pr (natural abundance 100%) has a nuclear spin of $I = 5/2$ and a nuclear magnetic moment of +4.3 nuclear magnetons. The spin Hamiltonian for the EPR spectrum of $Pr^{4+}/Ba_3CeIr_2O_9$ is:

$$H = g\beta\mathbf{H}\cdot\mathbf{S}' + A\mathbf{I}\cdot\mathbf{S}' - g'_N\beta\mathbf{H}\cdot\mathbf{I} \quad (1)$$

where g is the g value for Pr^{4+} with an effective spin $S' = 1/2$, A is the hyperfine coupling constant, g'_N is the effective nuclear g value (in units of Bohr magnetons), β is the Bohr magneton, and $\mathbf{H}$ is the applied magnetic field. Usually the assumption can be made that the electronic Zeeman term (the first term on the right-hand side of Eq. 1) is much larger than the hyperfine term (the second term on the right-hand side), which would result in a six-line spectrum for an isotropic resonance with $I = 5/2$. Ex-

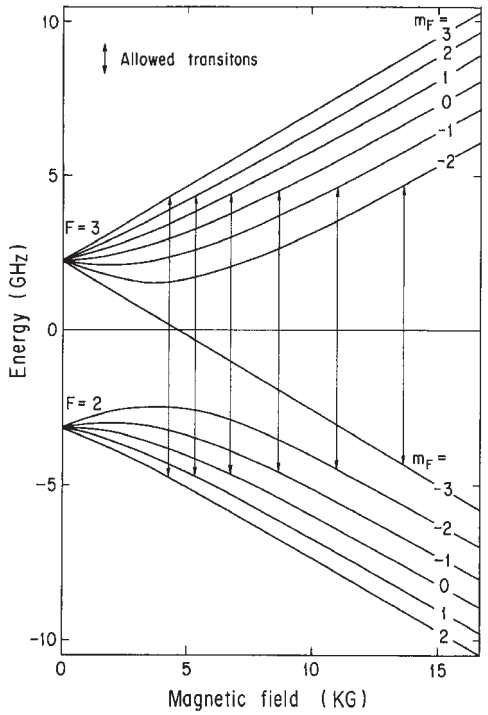

Fig. 4. Zeeman energy levels for Pr^{4+} ion in $Ba_3CeIr_2O_9$. Arrows show the observable EPR transitions at 4.2 K.

perimental results show that the observed hyperfine spacings between the absorption lines are quite large and that they increase with the magnetic field (see Fig. 3), which indicates that the electron spin quantum number and the nuclear spin quantum number are not good quantum numbers. In this case, the hyperfine interaction with the ^{141}Pr nucleus is so large that the spin Hamiltonian including the electronic Zeeman term and the hyperfine term must be solved exactly. The solution is well known (Breit–Rabi equation) and has been provided by Ramsey[20] and others.[21]

First, **I** and **S** are coupled together to form the resultant **F**, where $\mathbf{F} = \mathbf{I} + \mathbf{S}$. For $S = 1/2$ and $I = 5/2$ in the absence of a magnetic field, there are two states, $F = 2$ and $F = 3$, which are separated by $3A$. When the magnetic field is included, each of these two states splits into $(2F + 1)|m_F\rangle$ Zeeman levels, and six allowed transitions ($\Delta F = \pm 1$; $\Delta m_F = \pm 1$) should be observable (see Fig. 4). In order to obtain the g value and the hyperfine coupling constant A, we tried to fit the five observed resonance peaks to the calculated ones. The best fitting parameters are $|g| = 0.695$ and $A = 0.0606$ cm^{-1}. Table 2 lists the results of fitting the observed EPR spectra to the parameters of the spin Hamiltonian Eq. 1. The resonance field for the sixth transition (the highest resonance field) is calculated to be 13608 G, which is beyond our maximum obtainable magnetic field.

The g value for a $4f^1$ electron perturbed by the octahedral crystal field should be between $-10/7$ (no crystal field effect, for the Γ_7 ground doublet in the $^2F_{5/2}$ multiplet) and 2.00 (no spin–orbit interaction), and increases with increasing crystal field strength.[22,23] Although the sign of the g value was not obtained in this experiment, a comparison with other f^1 systems in octahedral symmetry, such as NpF_6/UF_6[24] and Pa^{4+}/Cs_2ZrCl_6,[21] indicates that the g value for the $Pr^{4+}/Ba_3CeIr_2O_9$ should be negative. Therefore, the value of $|g|$ which was obtained from the EPR experiment decreases with increasing crystal field strength. The $|g|$ value obtained for $Pr^{4+}/Ba_3CeIr_2O_9$ is 0.695, which is comparable to the values reported earlier for the Pr^{4+} ion in an octahedral coordination ($|g| = 0.64$–0.74), $Pr^{4+}/BaZr_xCe_{1-x}O_3$,[25] and much smaller than $|-10/7|$, indicating that the crystal field effect on the Pr^{4+} ion is strong. The effective magnetic moment of Pr^{4+} is calculated to be 0.602 μ_B from the relation $\mu = g\sqrt{S'(S'+1)}$. This moment is close to the moment of $Ba_3PrIr_2O_9$ (0.75(1) μ_B) derived from the magnetic susceptibility measurements.

Table 2. Experimental and Calculated EPR Absorption Line Positions for $Ba_3Pr_{0.05}Ce_{0.95}Ir_2O_9$[a)]

Experimental	Calculated[b)]	Difference
—	13608	—
10885	10879	6
8576	8535	41
6651	6648	3
5212	5215	−3
4040	4170	−130

a) All values are given in Gauss. b) Spin Hamiltonian parameters: $|g| = 0.695$, $A = 0.0606$ cm^{-1}, g'_N set equal to 0.0.

We have also measured the EPR spectrum for Pr^{4+} doped in $Ba_3CeRu_2O_9$. Fitting Eq. 1 to the experimental EPR spectra gives $|g| = 0.673$ and $A = 0.0606$ cm^{-1}. The situation for the Pr^{4+} ions in the $Ba_3CeIr_2O_9$ and in the $Ba_3CeRu_2O_9$ is the same, i.e., the central Pr^{4+} ion is almost octahedrally coordinated by six oxygens, but the crystal field strength is different between them. The average Pr^{4+}–O^{2-} distance in the $Pr^{4+}/Ba_3CeRu_2O_9$ is shorter than that in the $Pr^{4+}/Ba_3CeIr_2O_9$. Therefore, the strength of the crystal field affecting the electronic state of the central Pr^{4+} ion in the former compound should be stronger than that in the latter compound. The present experimental result indicated that the $|g|$ value for the $Pr^{4+}/Ba_3CeRu_2O_9$ is smaller than that for the $Pr^{4+}/Ba_3CeIr_2O_9$. This result is in accordance with the above theoretical consideration. On the other hand, the hyperfine coupling constant A is almost the same as those for the Pr^{4+} octahedrally coordinated by six oxygens.[4,25]

Summary

The magnetic properties of $Ba_3PrM_2O_9$ and $Ba_3CeM_2O_9$ (M = Ir, Ru) have been studied. The magnetic susceptibility of $Ba_3PrIr_2O_9$ shows that an antiferromagnetic interaction between two Ir ions in the Ir_2O_9 dimer results in the temperature-independent paramagnetism over the wide temperature range. The effective magnetic moments for $Ba_3PrIr_2O_9$ and $Ba_3PrRu_2O_9$ are very small, which were analyzed by the EPR measurements on the Pr^{4+} ions doped in the $Ba_3CeIr_2O_9$ and $Ba_3CeRu_2O_9$.

The present study was supported by the Japan Securities Scholarship Foundation.

References

1 N. E. Topp, "Chemistry of the Rare-Earth Elements," Elsevier, Amsterdam (1965).

2 Y. Hinatsu, *J. Solid State Chem.*, **100**, 136 (1992).
3 Y. Hinatsu, *J. Solid State Chem.*, **102**, 362 (1993).
4 Y. Hinatsu and N. Edelstein, *J. Solid State Chem.*, **112**, 53 (1994).
5 Y. Hinatsu, M. Itoh, and N. Edelstein, *J. Solid State Chem.*, **132**, 337 (1997).
6 K. Tezuka, Y. Hinatsu, Y. Shimojo, and Y. Morii, *J. Phys.: Condens. Matter*, **10**, 11703 (1998).
7 M. Itoh, K. Tezuka, M. Wakeshima, and Y. Hinatsu, *J. Solid State Chem.*, **145**, 104 (1999).
8 K. Itoh, K. Tezuka, and Y. Hinatsu, *J. Solid State Chem.*, **157**, 173 (2001).
9 R. D. Burbank and H. T. Evans, *Acta Crystallogr.*, **1**, 330 (1948).
10 Y. Doi, M. Wakeshima, Y. Hinatsu, A. Tobo, K. Ohoyama, and Y. Yamaguchi, *J. Mater. Chem.*, **11**, 3135 (2001).
11 Y. Doi, K. Matsuhira, and Y. Hinatsu, *J. Solid State Chem.*, **165**, 317 (2002).
12 Y. Doi and Y. Hinatsu, *J. Mater. Chem.*, **12**, 1792 (2002).
13 Y. Hinatsu, *J. Solid State Chem.*, **119**, 405 (1995).
14 F. Izumi and T. Ikeda, *Mater. Sci. Forum*, **321–324**, 198 (2000).
15 I. Thumm, U. Treiber, and S. Kemmler-Sack, *Z. Anorg. Allg. Chem.*, **477**, 161 (1981).
16 U. Treiber, S. Kemmler-Sack, A. Ehmann, H.-U. Schaller, E. Durrschmidt, I. Thumm, and H. Bader, *Z. Anorg. Allg. Chem.*, **481**, 143 (1981).
17 Y. Doi and Y. Hinatsu, *J. Phys.: Condens. Matter*, **16**, 2849 (2004).
18 Y. Hinatsu, M. Wakeshima, N. Edelstein, and I. Craig, *J. Solid State Chem.*, **144**, 20 (1999).
19 A. Abragam and B. Bleaney, "Electron Paramagnetic Resonance of Transition Ions," Oxford Univ. Press, London (1970), Chap. 5.
20 N. F. Ramsey, "Molecular Beams," Clarendon Press, Oxford (1956).
21 J. D. Axe, H. J. Stapleton, and C. D. Jeffries, *Phys. Rev.*, **121**, 1630 (1961).
22 Y. Hinatsu, T. Fujino, and N. Edelstein, *J. Solid State Chem.*, **99**, 182 (1992).
23 Y. Hinatsu, *J. Alloys Compd.*, **203**, 251 (1994).
24 C. A. Hutchison and B. Weinstock, *J. Phys. Chem.*, **32**, 56 (1960).
25 Y. Hinatsu, *J. Solid State Chem.*, **122**, 384 (1996).